

# Optimal Placement of Triaxial Accelerometers for Modal Vibration Tests

Daniel C. Kammer  
Department of Engineering Physics  
University of Wisconsin  
Madison, WI 53706

Michael L. Tinker  
Structural Dynamics and Loads Group  
Structures, Mechanics, and Thermal Department  
NASA/Marshall Space Flight Center  
Huntsville, AL 35812

## ABSTRACT

Proper pretest planning is a vital component of any successful vibration test. An extremely important part of the pretest exercise is the placement of sensors, usually in the form of accelerometers. The accelerometers must be placed such that all of the important dynamic information is obtained during the course of the test. The resulting sensor configuration must be optimal in some sense such that test resources are conserved. The state-of-the-practice is to select individual sensor location/directions from a candidate set based upon one of several available criteria. Triaxial accelerometers are then placed at the corresponding locations. In general, this results in the non-optimal placement of many of the accelerometers. This paper presents a new technique, based upon Effective Independence, that places triaxial accelerometers as single units in an optimal fashion. The technique is applied and compared with standard approaches using the X-33 vehicle.

## 1.0 INTRODUCTION

Proper pretest planning is a vital component of any successful vibration test. This is especially the case when testing modern complex aerospace structures. An extremely important part of the pretest exercise is the placement of sensors, usually in the form of accelerometers. The accelerometers must be placed such that all of the important dynamic information is obtained during the course of the test. At the same time, the resulting sensor configuration must be optimal in some sense such that testing resources are conserved. Quite often, the measure of goodness used to rate the utility of a sensor configuration is its ability to produce an accurate analytical representation containing degrees of freedom corresponding to the sensor locations. The reduced representation, called a Test-Analysis-Model (TAM), is used to perform test-analysis correlation [1]. The complexity of the sensor placement problem requires that it be automated in some fashion.

A great deal of research has been conducted over the last decade on optimal sensor placement using a variety of placement techniques and criteria. For example Salama et al. [2] proposed using modal kinetic energy as a means of

ranking the importance of candidate sensor locations. There have also been several variants on this theme, such as Average Kinetic Energy and Weighted Average Kinetic Energy (WAKE) proposed by Chung and Moore. [3]. A second approach using the mass-to-stiffness ratio associated with each candidate sensor location was proposed by Henshell and Ong [4]. Both of these techniques work well in conjunction with the Static Reduction technique for TAM generation [5]. However, modern finite element models have become so refined that the mass is smeared very evenly over the structure, making it difficult to select important degrees of freedom based on a mass weighting. Another method, called MAC, proposed by Carne and Dhormann [6], uses the minimization of the off-diagonal terms in the Modal Assurance Criterion matrix [1] as a measure of the utility of a sensor configuration. Techniques such as the genetic algorithm can also be used to search for optimal sensor configurations based upon a number of measures of goodness, such as the determinant of the Fisher information matrix [7] or the Modal Assurance Criterion matrix [8]. Far too many sensor placement approaches exist to mention them all in this paper.

Regardless of the approach used to place sensors, once the individual sensor location/directions are selected, the state-of-the-practice is to place triaxial accelerometers at the corresponding locations. This is done to simplify test setup and to benefit the visualization of the mode shapes. In general, this results in the non-optimal placement of many of the accelerometers. For example, if the x-direction at a particular location on the structure is selected, y- and z-direction accelerometers are also placed at the same point. This paper presents a new technique, based upon Effective Independence [9], that places triaxial accelerometers as single units in an optimal fashion. The technique is applied and compared with standard approaches using the X-33 advanced technology demonstrator vehicle for the Reusable Launch Vehicle program.

## 2.0 THEORY

The sensor placement technique presented in this paper is based on a previously developed technique called Effective Independence (*EfI*) [9]. The objective of this sensor

placement strategy is to select individual sensor locations which render the target mode shape partitions as linearly independent as possible while at the same time maximizing the signal strength corresponding to the target modal responses within the sensor data. Independence of the target mode partitions is required such that the test data can be used in test-analysis correlation as discussed previously. Signal strength is required to extract the target modes from the measured test data in the presence of noise. Obviously, the actual target modes are not available to aid the test engineer in placement of the sensors prior to the test. Instead, the next best thing is to place sensors with the aid of the FEM representation of the target modes partitioned to the sensor locations  $\phi_s$ . In the case of *EfI*, the sensor placement process begins by designating a large set of candidate sensor locations from which the smaller final sensor configuration will be selected. Modal kinetic energy can be used to help determine a good candidate sensor set.

As shown in Ref. [9], sensor placement can be cast in the form of an estimation problem with a corresponding Fisher information matrix given by

$$Q = \phi_s^T W \phi_s \quad (1)$$

in which  $W$  is a weighting matrix, such as the inverse of the sensor noise covariance matrix or a mass matrix. The modal response is estimated based upon the measured sensor data. Maximization of  $Q$  results in the minimization of the corresponding error covariance matrix which results in the best estimate. Sensors should be placed such that  $Q$  is maximized in an appropriate matrix norm. Maximization of the Fisher information matrix determinant is a commonly used criterion for optimal parameter estimation. It is also appropriate for optimal sensor placement. Maximizing the determinant of the information matrix will maximize the spatial independence of the target modal partitions and maximize the corresponding signal strength. The Effective Independence technique uses the determinant of the Fisher information matrix as a metric.

It has been shown that the Fisher Information matrix can be decomposed into the contributions from each candidate sensor location in the form

$$Q = \sum_{i=1}^{n_c} \phi_{si}^T \phi_{si} = \sum_{i=1}^{n_c} Q_i \quad (2)$$

where  $\phi_{si}$  is the  $i$ th row of the target mode partition matrix associated with the  $i$ th candidate sensor location,  $n_c$  is the number of candidate sensors, and the weighting has been taken as an identity matrix. It can be seen from Eq. (2) that as sensors are deleted from the candidate set, information is deleted from the Fisher information matrix. As shown in Refs. [10, 11], as the  $i$ th sensor is deleted, the determinant of the new Fisher information matrix  $Q^i$  can be expressed in terms of the original Fisher

information matrix as

$$\det(Q^i) = \det(Q) \det(1 - E_i) \quad (3)$$

where  $E_i$  is the Effective Independence value corresponding to the  $i$ th sensor given by

$$E_i = \phi_{si} Q^{-1} \phi_{si}^T \quad (4)$$

Equation (3) indicates that  $E_i$  represents the fractional reduction of the Fisher information matrix determinant if the  $i$ th sensor is deleted from the candidates sensor set. The candidate sensors can be ranked based upon their Effective Independence values. The sensor with the smallest value is deleted and the Effective Independence is calculated for the new candidate set. In an iterative fashion, the candidate set can be reduced to the desired number of sensors and the determinant of the Fisher information matrix can be maintained in a suboptimal way. Note that value of  $E_i$  lies in the range  $0 \leq E_i \leq 1$ . If the *EfI* value for a sensor is 0.0, the sensor can be deleted with no impact on the determinant of  $Q$ . If the *EfI* value is 1.0, the sensor is vital to the independence of the target modes and cannot be deleted from the candidate set. It is important to note that as a sensor is deleted from the candidate set, the *EfI* values change for the remaining sensors. In order to guarantee that a vital sensor is not thrown away during any iteration, the present formulation of the Effective Independence technique requires that only one sensor is thrown away at a time.

The goal of the work presented here is to reformulate Effective Independence such that uniaxial candidate sensor directions can be grouped and deleted by node. In general, candidate nodes will have six associated degrees of freedom, three translations and three rotations. However, the usual practice is to place triaxes at selected nodes to measure translational motion. Therefore, this paper considers only this case. The proposed technique can be easily generalized to the case of all six degrees of freedom. Instead of a candidate set of sensor locations, a candidate set of nodes with triaxes is chosen. Equation (2) can be modified to give

$$Q = \sum_{i=1}^{n_n} \phi_{3i}^T \phi_{3i} = \sum_{i=1}^{n_n} Q_{3i} \quad (5)$$

in which  $\phi_{3i}$  is the target modal matrix partitioned to the three rows corresponding to the  $i$ th node, and  $n_n$  is the number of candidate nodes. The Fisher information matrix with the  $i$ th node deleted can then be written as

$$Q^{3i} = Q - \phi_{3i}^T \phi_{3i} = Q \left[ I_k - Q^{-1} \phi_{3i}^T \phi_{3i} \right] \quad (6)$$

where  $I_k$  is a  $k$  dimensional identity matrix and  $k$  is the number of target modes. Following the same procedure used for individual sensors in Ref. [10], the determinant of

the Fisher information matrix with the  $i$ th node removed can be written as

$$\begin{aligned} \det(Q^{3i}) &= \det(Q) \det(I_3 - \phi_{3i} Q^{-1} \phi_{3i}^T) \\ &= \det(Q) \det(I_3 - E_{3i}) \end{aligned} \quad (7)$$

where  $E_{3i}$  is a  $3 \times 3$  fully populated matrix containing the  $E_{fl}$  values of the individual sensors corresponding to the  $i$ th node on the diagonal.

Equation (7) shows that the determinant of  $Q^{3i}$  reduces to zero and the target modes are no longer independent when  $E_{3i}$  possesses an eigenvalue  $\lambda = 1.0$ . This indicates that the  $i$ th node is vital to the independence of the target modes. Therefore, at least one of the three degrees of freedom associated with the  $i$ th node must have an  $E_{fl}$  value of 1.0. This statement can be proven by studying the form of  $E_{3i}$

$$\begin{aligned} E_{3i} &= \phi_{3i} Q^{-1} \phi_{3i}^T \\ &= \begin{bmatrix} \phi_{si1} Q^{-1} \phi_{si1}^T & \phi_{si1} Q^{-1} \phi_{si2}^T & \phi_{si1} Q^{-1} \phi_{si3}^T \\ \phi_{si2} Q^{-1} \phi_{si1}^T & \phi_{si2} Q^{-1} \phi_{si2}^T & \phi_{si2} Q^{-1} \phi_{si3}^T \\ \phi_{si3} Q^{-1} \phi_{si1}^T & \phi_{si3} Q^{-1} \phi_{si2}^T & \phi_{si3} Q^{-1} \phi_{si3}^T \end{bmatrix} \end{aligned} \quad (8)$$

in which  $\phi_{sir}$  is the  $r$ th row ( $r = 1, 2, 3$ ) from the target mode partition corresponding to the  $i$ th node. Without loss of generality, let the first degree of freedom from the  $i$ th node be critical to the independence of the target modes. The (1,1) term in  $E_{3i}$  gives the corresponding  $E_{fl}$  value

$$\phi_{si1} Q^{-1} \phi_{si1}^T = 1 \quad (9)$$

Premultiplying both sides of Eq. (9) by  $\phi_{si1}^T$  produces

$$\phi_{si1}^T \phi_{si1} Q^{-1} \phi_{si1}^T = P_{i1} \phi_{si1}^T = \phi_{si1}^T \quad (10)$$

The matrix  $P_{i1}$  is an oblique projector [12] onto the column space spanned by the vector  $\phi_{si1}^T$ . Equation (5) can be decomposed into the form

$$Q = \sum_{i=1}^{n_n} \sum_{r=1}^3 Q_{3ir} = \sum_{i=1}^{n_n} \sum_{r=1}^3 \phi_{sir}^T \phi_{sir} \quad (11)$$

Premultiplying  $Q$  by the oblique projector gives

$$P_{i1} Q = \phi_{si1}^T \phi_{si1} Q^{-1} Q = \phi_{si1}^T \phi_{si1} = Q_{3i1} \quad (12)$$

Equation (11) then implies that

$$P_{i1} Q_{3i2} + P_{i1} Q_{3i3} + \sum_{\substack{j=1 \\ j \neq i}}^{n_n} \sum_{r=1}^3 P_{i1} Q_{3jr} = 0 \quad (13)$$

By definition, matrices  $P_{i1}$  and  $Q_{3jr}$  are positive semidefinite, therefore, their product is also positive semidefinite. The terms in the sum of Eq. (13) must then vanish individually, yielding

$$P_{i1} Q_{3ir} = 0 \quad r \neq 1 \quad (14)$$

It can be shown that the columns of  $Q_{3jr}$  are parallel to the vector  $\phi_{sir}^T$ , therefore

$$P_{i1} \phi_{sir}^T = \phi_{si1}^T \phi_{si1} Q^{-1} \phi_{sir}^T = \phi_{si1}^T a_r = 0 \quad r \neq 1 \quad (15)$$

By definition,  $\phi_{si1}$  is nonzero, implying

$$a_r = \phi_{si1} Q^{-1} \phi_{sir}^T = 0 \quad r \neq 1 \quad (16)$$

The form of  $E_{3i}$  reduces to

$$E_{3i} = \begin{bmatrix} 1 & 0 & 0 \\ 0 & \phi_{si2} Q^{-1} \phi_{si2}^T & \phi_{si2} Q^{-1} \phi_{si3}^T \\ 0 & \phi_{si3} Q^{-1} \phi_{si2}^T & \phi_{si3} Q^{-1} \phi_{si3}^T \end{bmatrix} \quad (17)$$

which obviously has an eigenvalue of 1.0.

Therefore, if one of the sensor directions associated with the  $i$ th node is vital to the independence of the target modes,  $E_{3i}$  has an eigenvalue of 1.0 and the determinant of  $I_3 - E_{3i}$  becomes zero. Conversely, if  $\phi_{3i} \equiv 0$ , the determinant of  $I_3 - E_{3i}$  is 1.0 and Eq. (7) indicates that deleting the  $i$ th node has no impact on the determinant of the Fisher information matrix. The range of values which the determinant of  $I_3 - E_{3i}$  can take on can be determined by studying the expression in Eq. (7). The Fisher information matrix  $Q$  is positive definite, while  $Q^{3i}$  is at least positive semidefinite. The expression  $I_k - Q^{-1} \phi_{3i}^T \phi_{3i}$  must then be at least positive semidefinite. The eigenvalues of  $I_k - Q^{-1} \phi_{3i}^T \phi_{3i}$  can be expressed in the form

$$\lambda(I_k - Q^{-1} \phi_{3i}^T \phi_{3i}) = 1 - \lambda(Q^{-1} \phi_{3i}^T \phi_{3i}) \quad (18)$$

The sign definiteness of  $I_k - Q^{-1} \phi_{3i}^T \phi_{3i}$  then requires that  $\lambda(Q^{-1} \phi_{3i}^T \phi_{3i}) \leq 1$ . Based on its form,  $Q^{-1} \phi_{3i}^T \phi_{3i}$  is also positive semidefinite. Therefore, the eigenvalues of  $Q^{-1} \phi_{3i}^T \phi_{3i}$  must satisfy the inequality

$$0 \leq \lambda(Q^{-1} \phi_{3i}^T \phi_{3i}) \leq 1 \quad (19)$$

which then implies that

$$0 \leq \lambda(I_k - Q^{-1} \phi_{3i}^T \phi_{3i}) \leq 1 \quad (20)$$

Using this result, Eq. (7) shows that the range on the determinant of  $I_3 - E_{3i}$  is given by

$$0 \leq \det(I_3 - E_{3i}) \leq 1 \quad (21)$$

A Triaxial Effective Independence measure ( $EfI3$ ) is then given by the expression

$$EfI3_i = 1 - \det(I_3 - E_{3i}) \quad (22)$$

with a range in values of  $0 \leq EfI3_i \leq 1$ . The value  $EfI3_i$  represents the fractional change in the determinant of the Fisher information matrix if the  $i$ th node is deleted from the candidate set. If a node is vital to target mode independence, the corresponding  $EfI3$  value is 1.0, and if the node contributes nothing to the independence, its  $EfI3$  value is 0.0. Using this measure, the candidate node set can be ranked, sorted, and the lowest ranked node deleted. In an iterative fashion, the candidate set of nodes can be paired down to the desired number of triaxes for modal testing.

### 3.0 APPLICATION TO X-33 VEHICLE

The X-33, shown in Fig. 1, is an advanced technology demonstrator vehicle for the Reusable Launch Vehicle program. The finite element model, obtained from Marshall Space Flight Center (MSFC), is illustrated in Fig. 2. It contains 16,653 nodes, 28,050 elements, and produces 830 modes with frequencies below 55.0 Hz. Twenty seven target modes were selected by MSFC for the empty X-33 vehicle within this frequency range. Modes with frequencies below 25.0 Hz. are termed vehicle modes while those above 25.0 Hz. are termed control surface modes in accordance with Ref. [13]. The vehicle modes are listed in Table 1 along with some descriptions. Typical modes are illustrated in Figs. 3 and 4. In the following analyses, no effort was made to remove any translational degrees of freedom that physically cannot be used for sensor placement from any of the candidate sensor sets.

An initial candidate set of sensor locations was selected based upon modal kinetic energy. A set of triaxes was selected at 3,277 nodes. This candidate set of 9,831 degrees of freedom provided essentially 100.0 percent of the kinetic energy for each of the target modes. Initially, the straightforward Effective Independence approach which deletes one sensor location at a time was applied to the initial candidate set. The set was iteratively reduced to 400 sensor locations. These locations were distributed over 389 nodes. Additional sensors were then added to complete triaxes at each of the corresponding nodes, producing 1167 total sensors. The added 767 sensors are nonoptimal with respect to the determinant of the Fisher information matrix. The corresponding determinant value is 9.38e38. The new Triaxial Effective Independence approach was then applied to the same initial candidate set of nodes. Nodes were deleted in an iterative fashion until the optimum 389 nodes remained. The resulting Fisher

information matrix had a determinant of 1.78e39. Figure 5 shows that the Triaxial Effective Independence technique tends to maintain the determinant of the Fisher information matrix as nodes are deleted.

A second analysis was then performed using the same initial candidate set of sensors. This time the uniaxial Effective Independence technique was applied to reduce the candidate set to 200 individual sensors distributed over 195 nodes. Additional sensors were added to complete each triax to produce 585 total sensors. This sensor configuration produced a Fisher information matrix determinant of 2.42e32. The corresponding analysis was then performed using Triaxial Effective Independence. The selected 195 nodes produced a determinant value of 6.02e32. In each case, the larger Fisher information matrix determinant implies that the corresponding sensor configuration produced by the Triaxial Effective Independence technique will provide better estimates of the target mode shapes and frequencies.

As mentioned previously, it is also important for the selected sensor configuration to produce an accurate TAM for test-analysis correlation. There are several different types of TAM representations to choose from, but in many cases, the standard is still the TAM produced by the static or Guyan reduction [5]. In order for Effective Independence based sensor configurations to produce an accurate static TAM, the mass matrix must be used as weighting in the generation of the Fisher information matrix in Eq. (1). The most accurate approach would be to premultiply the target modes partitioned to the initial candidate sensor by the square root of the corresponding FEM mass matrix, rank and delete the least important sensor or node, and then statically reduce the mass matrix to the new candidate sensor set. For large candidate sensor sets, this approach can become computationally intensive. Instead, in this analysis, the target modes were weighted only initially by the square root of the diagonal of the mass matrix. The modes were then not reweighted by a new mass matrix after each iteration. This approach provides the correct initial mass weighting, but does not account for redistribution of the mass as sensor locations are deleted from the candidates set.

The uniaxial Effective Independence technique was applied to the mass weighted target modes to reduce the candidate sensor set to 430 locations which were distributed over 391 nodes. As before, triaxes were then completed at each node, producing 1173 total sensor locations. The Triaxial Effective Independence technique was then applied to the same mass weighted target modes. The candidate set of nodes was iteratively reduced to 389. Each sensor configuration was used to generate a static TAM which produced a corresponding set of mass normalized mode shapes and frequencies. Cross-orthogonality

$$C = \phi_s^T M_{TAM} \phi_{TAM}$$

was used to match and compare FEM and TAM mode shapes. A cross-generalized mass of 1.0 would correspond

to a perfect match of the mode shapes. The criteria used for accurate correlation in this work is a cross-generalized mass value greater than or equal to 0.90 and a corresponding frequency error less than or equal to 5.0%. Neither of the TAMs predicted any of the target modes above 25.0 Hz., therefore the remaining analysis considers only the 17 vehicle modes below 25.0 Hz. Figure 6 presents the target mode cross-generalized mass values for each of the TAM representations. Figure 7 shows the corresponding frequency errors. The Efi based TAM accurately predicted nine of the target modes, while the Efi3 based TAM accurately predicted eleven of the target modes. The average cross-generalized mass value over all 17 of the target modes was 0.87 for the Efi TAM and 0.91 for the Efi3 based TAM. These results show that the sensor configuration based on Triaxial Effective Independence produced a more accurate TAM representation, even though it possessed six fewer sensors.

Finally, the Efi3 based TAM was compared to a TAM representation containing 389 triaxes generated by MSFC using a combination of weighted average kinetic energy, mass-to-stiffness ratios, and engineering judgment. Figure 8 compares the cross-generalized mass values, while Fig. 9 compares the frequency errors. According to the stated accuracy criteria, the MSFC TAM predicts nine of the 17 target modes with an overall average cross-generalized mass value of 0.84. The Efi3 based TAM predicts all the target modes predicted by the MSFC TAM with the exception of elastic mode 84, but in addition, predicts elastic modes 12, 15, and 16. Considering the overall cross-generalized mass values and frequency errors, the mass weighted Efi3 based sensor configuration produces the more accurate TAM. Note that the MSFC TAM also did not accurately predict any of the target modes above 25.0 Hz.

## 5.0 CONCLUSION

A new method based upon Effective Independence has been presented for the placement of triaxial sensors for a modal vibration test. The state-of-the-practice is to select individual sensor location/directions from a candidate set based upon one of several available criteria. Triaxial accelerometers are then placed at the corresponding locations for the vibration test. In general, this results in the non-optimal placement of many of the accelerometers. The new technique, called Triaxial Effective Independence, is an improvement in that it places triaxial accelerometers as single units in an optimal fashion. The technique was applied to identify 27 target modes for the X-33 advanced technology demonstrator vehicle. Triaxial sensor configurations produced by the Triaxial Effective Independence technique consistently produced larger Fisher information matrix determinants than configurations generated by expanding uniaxial Effective Independence results. In addition, a static TAM generated using mass weighted Triaxial Effective Independence was compared with a TAM produced by the uniaxial Effective Independence technique and a TAM produced using a combination of weighted average kinetic energy, mass-to-

stiffness ratios, and engineering judgment. In each case, the Triaxial Effective Independence sensor configuration predicted more target modes with greater accuracy.

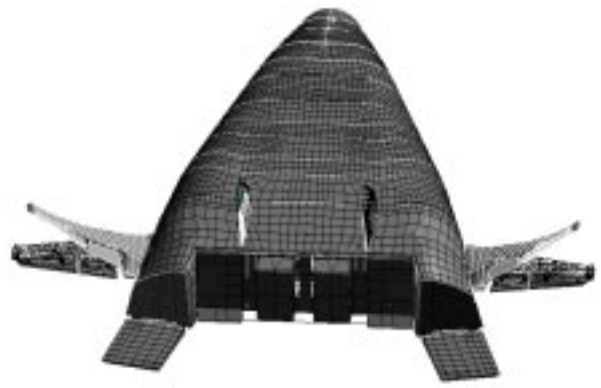
## ACKNOWLEDGMENTS

This work was supported by NASA Marshall Space Flight Center under Grant NAG8-1820.

## REFERENCES

- [1] Friswell, M. I. and J. E. Mottershead, "Finite Element Model Updating in Structural Dynamics," edited by G. M. L. Gladwell, Kluwer Academic Publishers, Dordrecht, 1995, pp. 56-77.
- [2] Salama, M., T. Rose and J. Garba, "Optimal Placement of Excitations and Sensors for Verification of Large Dynamical Systems," *28th Structures, Structural Dynamics, and Materials Conference*, Monterey, CA, 1987, pp. 1024-31.
- [3] Chung, Y. T. and J. D. Moore, "On-Orbit Sensor Placement and System Identification of Space Station with Limited Instrumentations," *11th International Modal Analysis Conference*, Kissimmee, FL, 1993, pp. 41-46.
- [4] Henshell, R. D. and J. H. Ong, "Automatic Masters for Eigenvalue Economization," *Earthquake Engineering and Structural Dynamics*, **3**, 1975, pp. 375-383.
- [5] Guyan, R. J., "Reduction of Mass and Stiffness Matrices," **3**(2), 1965, pp. 380.
- [6] Carne, T. G. and C. R. Dhormann, "A Modal Test Design Strategy for Model Correlation," *13th International Modal Analysis Conference*, Nashville, TN, 1995.
- [7] Yao, L., W. A. Sethares and D. C. Kammer, "Sensor Placement for On-Orbit Modal Identification via a Genetic Algorithm," *AIAA Journal*, **31**(10), 1993, pp. 1922-1928.
- [8] Stabb, M. and P. Blesloch, "A Genetic Algorithm for Optimally Selecting Accelerometer Locations," *13th International Modal Analysis Conference*, , 1995, pp. 1530-1534.
- [9] Kammer, D. C., "Sensor Placement for On-Orbit Modal Identification and Correlation of Large Space Structures," *Journal of Guidance, Control, and Dynamics*, **14**(2), 1991, pp. 251-259.
- [10] Kammer, D. C. and L. Yao, "Enhancement of On-Orbit Modal Identification of Large Space Structures through Sensor Placement," *Journal of Sound and Vibration*, **171**(1), 1994, pp. 119-140.

- [11] Poston, W. L. and R. H. Tolson, "Maximizing the Determinant of the Information Matrix with the Effective Independence Method," *Journal of Guidance, Control, and Dynamics*, **15**(6), 1992, pp. 1513-1514.
- [12] Greville, T. N. E. and A. Ben-Israel, *Generalized Inverses: Theory and Applications*, Wiley, New York, NY, 1974.
- [13] Bedrossian, H., M. L. Tinker, and H. Hidalgo, "Ground Vibration Test Planning and Pre-Test Analysis for the X-33 Vehicle," AIAA Paper No. 2000-1586, 2000.



Canted Fin Symmetric Bending (6.41 Hz)

Fig. 3. X-33 vehicle elastic mode 1.

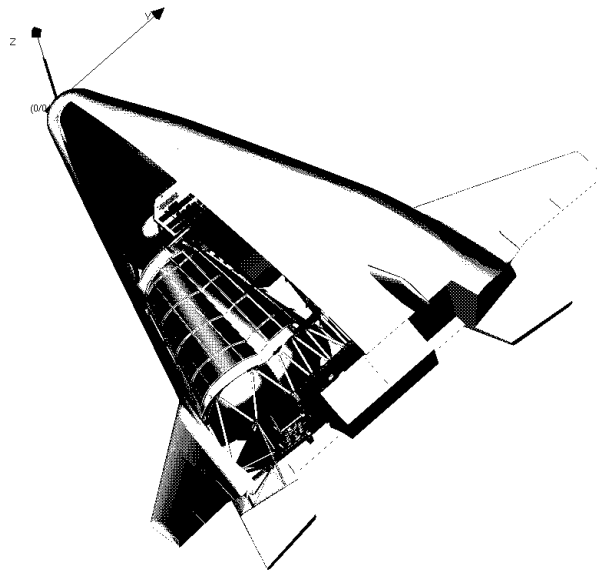


Fig. 1. X-33 vehicle.

Table 1. X-33 empty vehicle target modes.

Elastic Mode No.	Freq. Hz.	Description
1	6.41	Canted fin sym. bending
3	6.91	Canted fin anti-sym. bending
4	8.32	Vehicle torsion + LOX frame
11	10.20	Body flap anti-sym
12	10.44	Body flap sym
15	10.90	Vehicle normal (Z) bending + avionics bay + body flap
16	11.00	Vehicle yaw (LOX tank)
21	11.42	Vehicle yaw
22	11.88	Vehicle yaw + frame 6&7 + canted fin
23	11.99	Canted fin in-plane: sym
46	14.14	Vehicle Z bending
68	16.75	Vertical fin anti-symmetric
71	16.97	Vertical fin symmetric
75	17.84	None
81	18.35	None
83	18.54	None
84	18.58	None

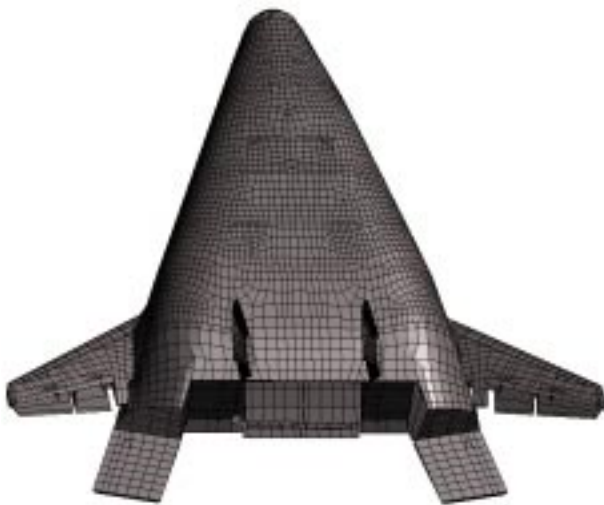


Fig. 2. X-33 vehicle finite element model representation.



Vehicle Yaw (11.0 Hz)

Fig. 4. X-33 vehicle elastic mode 16.

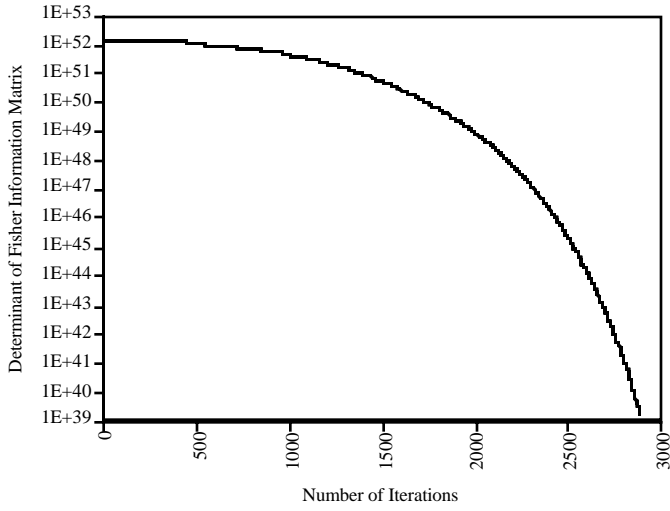


Fig. 5. Fisher information determinant using Efi3.

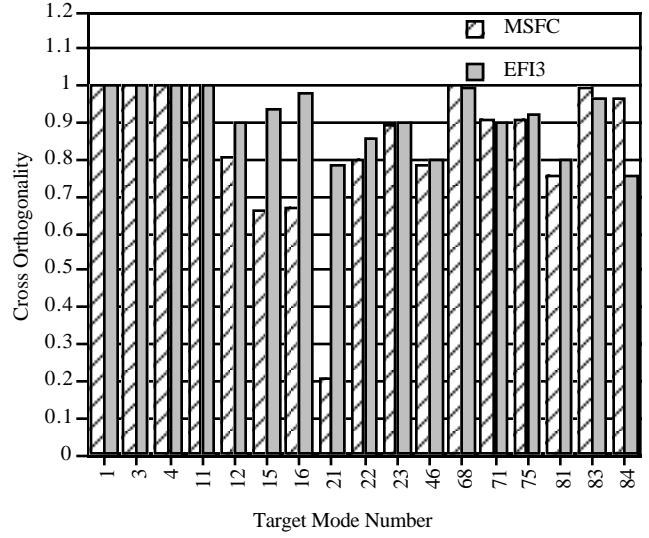


Fig. 8. Cross-orthogonality for MSFC and Efi3 TAMs.

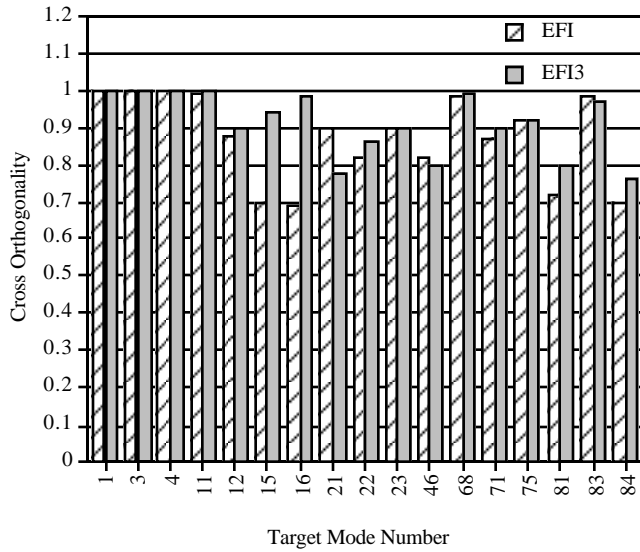


Fig. 6. Cross-orthogonality for Efi and Efi3 TAMs.

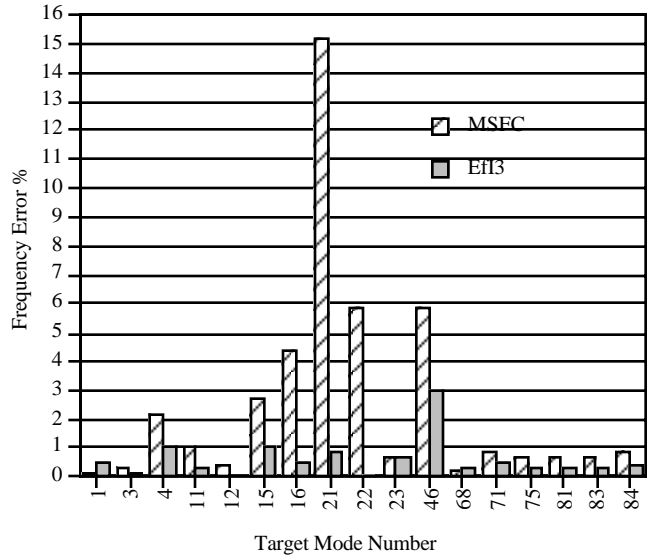


Fig. 9. Frequency error for MSFC and Efi3 TAMs.

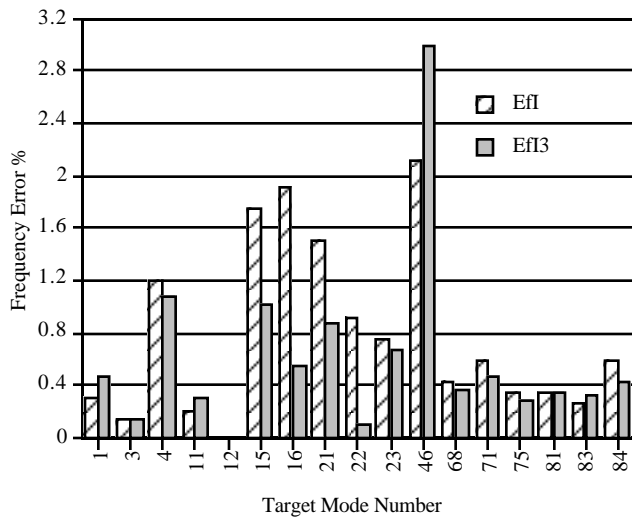


Fig. 7. Frequency error for Efi and Efi3 TAMs.